

# JGR Space Physics

## RESEARCH ARTICLE

10.1029/2019JA026582

### Key Points:

- It is the first time to investigate and find the north-south hemispheric asymmetry of FAE distribution in the two cusps
- The asymmetry appeared in total FAE number, distribution versus altitude and ILAT, both for up and down directions
- It is important to understand the physics mechanism of the particles distribution and dynamics in the cusps and magnetosphere

### Correspondence to:

Z. Zhang,  
zhangziying0501@sina.com

### Citation:

Shi, J., Zhang, Z., Torkar, K., Cheng, Z., Escoubet, P., Farzakeley, A., et al (2019). South-north hemispheric asymmetry of the FAE distribution around the cusp region: Cluster observation. *Journal of Geophysical Research: Space Physics*, 124, 5342–5352.  
<https://doi.org/10.1029/2019JA026582>

Received 31 JAN 2019

Accepted 21 JUN 2019

Accepted article online 30 JUN 2019

Published online 16 JUL 2019

## South-North Hemispheric Asymmetry of the FAE Distribution Around the Cusp Region: Cluster Observation

Jiankui Shi<sup>1,2</sup> , Ziyang Zhang<sup>3</sup> , Klaus Torkar<sup>4</sup> , Zhengwei Cheng<sup>1</sup> , Phillipe Escoubet<sup>5</sup>, Andrew Farzakeley<sup>6</sup>, Malcolm Dunlop<sup>7</sup> , and Chris Carr<sup>8</sup> 

<sup>1</sup>State Key Laboratory of Space Weather, National Space Science Center, Chinese Academy of Sciences, Beijing, China, <sup>2</sup>Schools of Astronomy and Space Science, University of Chinese Academy of Sciences, Beijing, China, <sup>3</sup>College of Applied Arts and Science of Beijing Union University, Beijing, China, <sup>4</sup>Space Research Institute, Austrian Academy of Sciences, Graz, Austria, <sup>5</sup>Scientific Support Office, ESA/ESTEC, Noordwijk, The Netherlands, <sup>6</sup>MSSL, University College London, London, UK, <sup>7</sup>SSTO, Rutherford Appleton Laboratory, Didcot, UK, <sup>8</sup>Imperial College London, London, UK

**Abstract** Cluster data from late July to early October were used to study the distribution of field-aligned electron (FAE) events around the two cusps. An FAE event was defined as electron parallel flux  $> 3 \times 10^8 \text{ (cm}^2 \text{ s)}^{-1}$ . The total number of FAE events around the two cusps was basically identical, but downward FAE events prevailed in the south and upward FAE events in the north. In the southern cusp, the peak of the FAE events distribution versus altitude was about  $1.3 R_E$  higher and the peak of the FAE events distribution versus invariant latitude (ILAT) was about  $4^\circ$  ILAT lower. Only the downward FAEs around the southern cusp had a second ILAT peak, which was located about  $11^\circ$  higher than the main peak. The normalized number of FAEs showed nearly the same features as the unnormalized number of the FAEs events. These results indicated a north-south asymmetry of the FAE distribution around the two cusps. Some causes for the asymmetry are discussed, the main ones being the asymmetry of the magnetospheric configuration resulting from geomagnetic dipolar tilt and solar wind flows, the interplanetary magnetic field asymmetry related to the magnetosphere, and the difference of ionospheric conductivity in the two hemispheres. Various solar wind-magnetosphere interaction processes, such as quasi-viscous interaction and reconnection, are responsible for the asymmetry, too. The second distribution peak (at higher ILAT) of the downward FAE events around the southern cusp corresponded to high solar wind speed and may be associated with the northward interplanetary magnetic field  $B_z$  field-aligned current at low altitude. This requires further studies, however.

## 1. Introduction

Many satellite observations show that field-aligned electrons (FAEs) can exist in various regions in the Earth's magnetosphere, such as the auroral zone, cusp/cleft region, polar cap region, and plasma sheet in the magnetotail (Carlson et al., 1998; Collin et al., 1982; Johnstone et al., 1994; Ma et al., 2009). The FAEs in the different regions have different characteristics.

FAEs are very important to solar wind-magnetosphere-ionosphere coupling and are associated with the field-aligned current (FAC) and the particle dynamics in the magnetosphere. As early as in the 1960s, polar electrons with pitch angle distributions peaking near  $0^\circ$  were observed by the OGO 4 satellite with 908-km apogee and 412-km perigee (Hoffman & Evans, 1968), which is the first observation of FAEs. Thereafter, with more satellite observations, more characteristics of FAEs in the polar region have been obtained. Some authors pointed out that both the upward and downward electrons could exist simultaneously in the polar region (Johnstone & Winningham, 1982; Lin & Hoffman, 1979; Sharp et al., 1980).

In the cusp region, upward FAEs were first observed at an altitude of about 1,800 km in the Southern Hemisphere by the Hawkeye 1 satellite in 1978, showing that the electron energy in the cusp region was concentrated in the range of 100–200 eV (Kintner et al., 1978). Subsequent studies have found upward and downward FAEs with pitch angles less than  $15^\circ$  in a spatial interval of several hundred kilometers in the satellite orbit altitude range of 1–4  $R_E$  in the cusp region, which was a common phenomenon there (Burch et al., 1983; Torbert & Carlson, 1980). FAEs in the range from 20 to 200 eV were a common

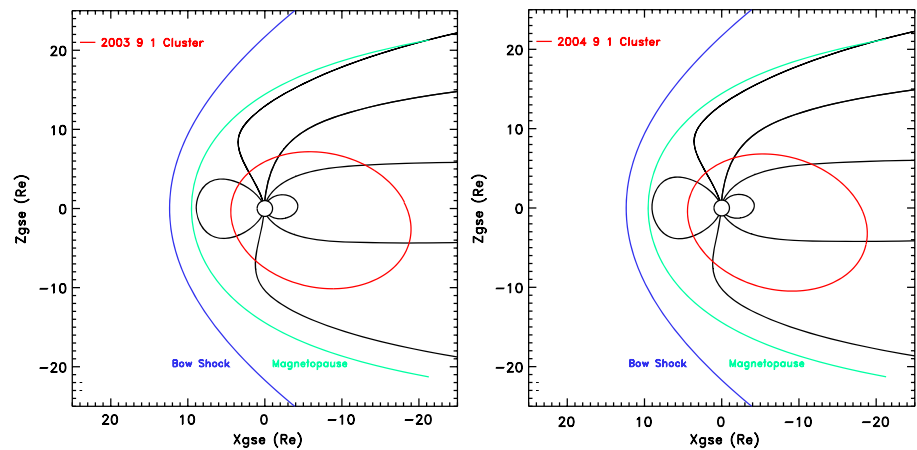


**Figure 1.** Example of Cluster orbit crossing the north and south cusps on 1 September in 2003 and 2004, respectively.

feature, and the maximum energy of these FAEs can reach several hundred electron volts at 287-km altitude in the southern cusp (Zanetti et al., 1981).

There were also some statistical results on the FAEs in the auroral zone and the polar cusp region. An earlier statistical study on FAEs was performed using the OGO 4 data. It showed that the occurrence of polar FAEs covers the entire auroral zone with the highest incidence near midnight at 70° invariant latitude (ILAT; Berko, 1973). The data from the satellite S3-3 were used to analyze the distribution of FAEs in ILAT and magnetic local time (MLT) at 3,000- to 8,000-km altitude in the polar region. It was found that the ILAT ranges from 63° to 81° and that the MLT distribution had two peaks, one at 07:00 in the morning and the other at 22:00 at night (Collin et al., 1982). Other statistical studies have also shown that the incidence of FAEs on the dawnside was larger than that on the duskside and that the FAEs in both directions were centralized on the dayside (Miyake et al., 1998; Thelin & Lundin, 1990).

Using the Cluster data, some authors reported that the duration of FAEs observed in the dayside polar region was within 60 s (Hu et al., 2008). Other authors have found that the duration of the FAE events could reach 475 s and most of the durations were within 40 s (Shi et al., 2014, 2017).

All the previous studies have provided some features of the FAE distribution in the polar region. However, there is no comparative study on the FAE distribution around the cusp region between the two hemispheres. Indeed, the Cluster satellites with their polar orbit provide a good opportunity to perform such a comparative study. Therefore, in this work, we use the Cluster data from 2003 and 2004 to study the FAE distribution around the cusp region in the Northern and Southern Hemispheres. Our results suggest a north-south asymmetry in the FAE distribution around the two cusps.

## 2. Data and Instrument

The Cluster mission comprises four satellites, which initially achieved a quasi-polar orbit with 19.7  $R_E$  apogee and 4  $R_E$  perigee (Escoubet et al., 2001). The satellites cross the cusp at the altitude of 4–8  $R_E$  both in the Southern and Northern Hemispheres from July to October in each year. Onboard Cluster, the instrument Plasma Electron And Current Experiment (PEACE) measures electron distributions in all directions within the energy range of 0.7 eV to 30 keV (Johnstone et al., 1997), and the FluxGate Magnetometer (FGM) measures the magnetic field in three components (Balogh et al., 2001). In this research, PEACE and FGM data from the Cluster C3 satellite in 2003 and 2004 are used. All the data are spin averages and have a time resolution of about 4 s. The data are from the Cluster Science Archive (<https://www.cosmos.esa.int/web/csa>). Figure 1 gives an example of the Cluster orbit crossing the northern and southern cusps on 1 September in 2003 and 2004, respectively. In each year from July to October the Cluster orbit was well suited to study on the two cusps.

In order to compare the characteristics of FAEs around the southern and northern cusps, we perform a statistical study on FAE distribution. According to the previous study (Shi et al., 2017), the FAEs in the polar

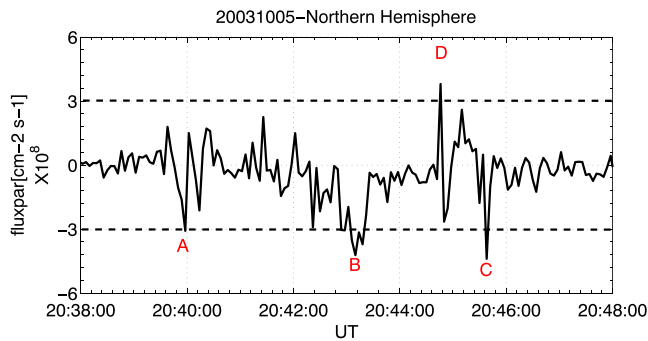


**Figure 2.** An example of the field-aligned electron events selection with the data from Cluster C3 on 5 October 2003. Two horizontal dashed lines mark the threshold of field-aligned electron flux.

region were distributed around the auroral oval with two peaks. One peak concentrated around the cusp region and the other concentrated in the premidnight zone in the both hemispheres. This study focuses on the north-south asymmetry of FAEs distribution around the cusp region, which is limited to MLT 0900–1500 and ILAT > 60°. The calculation method of MLT adopts the Tsyganenko T96-01 model (Tsyganenko & Stern, 1996).

In the early days, the FAEs were defined as the electrons moving along the magnetic field line, which was also called the “electron beam” (Carlson et al., 1998; Johnstone & Winningham, 1982). Indeed, electrons generally move with parallel and perpendicular velocity components relative to the magnetic field line. The Northern and Southern Hemispheres differ by the orientation of the geomagnetic field; upward electrons in the Northern and Southern Hemispheres have pitch angles near 180° and 0°, respectively. The electron field-aligned flux is given by the product of electron density and electron field-aligned velocity component, and the FAE events are determined from this accordingly.

We define the FAE as electrons with a significant parallel velocity component which can point upward or downward. To avoid the background noise, only electrons with field-aligned flux greater than  $3 \times 10^8 \text{ (cm}^2 \text{ s)}^{-1}$  were selected as FAE event in the analysis. Figure 2 gives an example of the event selection from the data. The two horizontal dashed lines mark the thresholds of the field-aligned flux at  $3 \times 10^8 \text{ (cm}^2 \text{ s)}^{-1}$  and  $-3 \times 10^8 \text{ (cm}^2 \text{ s)}^{-1}$ , respectively. Since this observation is in the Northern Hemisphere, a downward electron event has a positive value of the field-aligned flux. So we can see that there are three upward FAE events (A, B, and C) and one downward FAE events (D) in Figure 2.

### 3. Statistical Results

According to the condition of flux magnitude greater than  $3 \times 10^8 \text{ (cm}^2 \text{ s)}^{-1}$ , 712 FAE events were identified around the two cusp regions, 392 FAE events in the Southern Hemisphere, and 320 FAE events in the Northern Hemisphere.

The FAE events are divided into the upward and downward types. Some authors have studied the upward and downward flowing electrons in the polar region (Shi et al., 2017; Yoshioka et al., 2000). The downward FAEs mainly consist of the entering solar wind electrons, with possible contributions of upward ionospheric electrons reflected downward by the potential drop above the satellite. Therefore, the downward FAEs should mainly be located at higher altitudes. The upward FAE events are mainly composed of upflowing ionospheric electrons or entering solar wind electrons mirrored upward due to the gradually increasing magnetic field. Therefore, the upward FAEs should mainly be found at lower altitudes.

Figure 3 illustrates the distributions of the upward and downward FAE events around the two cusps in the MLT-ILAT plane. The left panel is for the Southern Hemisphere, and the right one is for the Northern Hemisphere

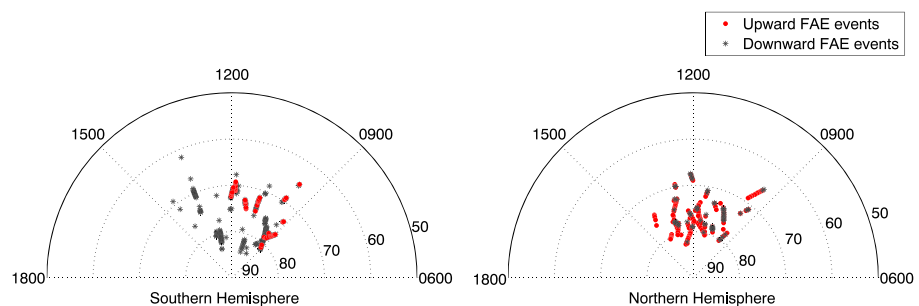


**Figure 3.** The upward and downward field-aligned electron (FAE) events distribution in the magnetic local time-invariant latitude plane in the two cusps. The left panel is for the Southern Hemisphere, and the right is for the Northern Hemisphere. The red symbols mark the upward, and the black symbols the downward FAE events.

**Table 1**  
Number of FAE Events in Both Hemispheres

Hemisphere	Upward FAE events	Downward FAE events	Total
Southern Hemisphere	75	317	392
Northern Hemisphere	243	77	320
Total	318	394	712

Note. FAE = field-aligned electron.

Hemisphere. The red symbols mark the upward and the black symbols the downward FAE events. From Figure 3, we can see a clear north-south asymmetry of the FAE events distribution versus ILAT around the two cusps. The asymmetry appeared both with MLT and ILAT direction. Indeed, the asymmetry also appeared with altitude distribution, which will be shown later.

### 3.1. Number of FAE Events Around Both Cusps

The number of selected FAE events in upward and downward direction in the northern cusp and southern cusp is shown in Table 1. The total number of FAE events observed around the southern cusp is slightly higher than that around the northern cusp. Also, the total number of upward FAE events is slightly less than that of the downward FAE events.

However, we can see that around the southern cusp region the number of the downward FAE events was about 4–5 times the number of upward events, and around the northern cusp region the number of the upward FAE events was about 3–4 times the number of downward events. That is, to say, the FAE events around the cusp regions, both the upward and downward ones, had an asymmetric occurrence in the Southern and Northern Hemispheres.

### 3.2. Altitude Distribution in Both Hemispheres

The upper and middle panels in Figure 4 show the FAEs distribution (with event number and normalized number) versus altitude in upward and downward direction around the northern and the southern cusp.

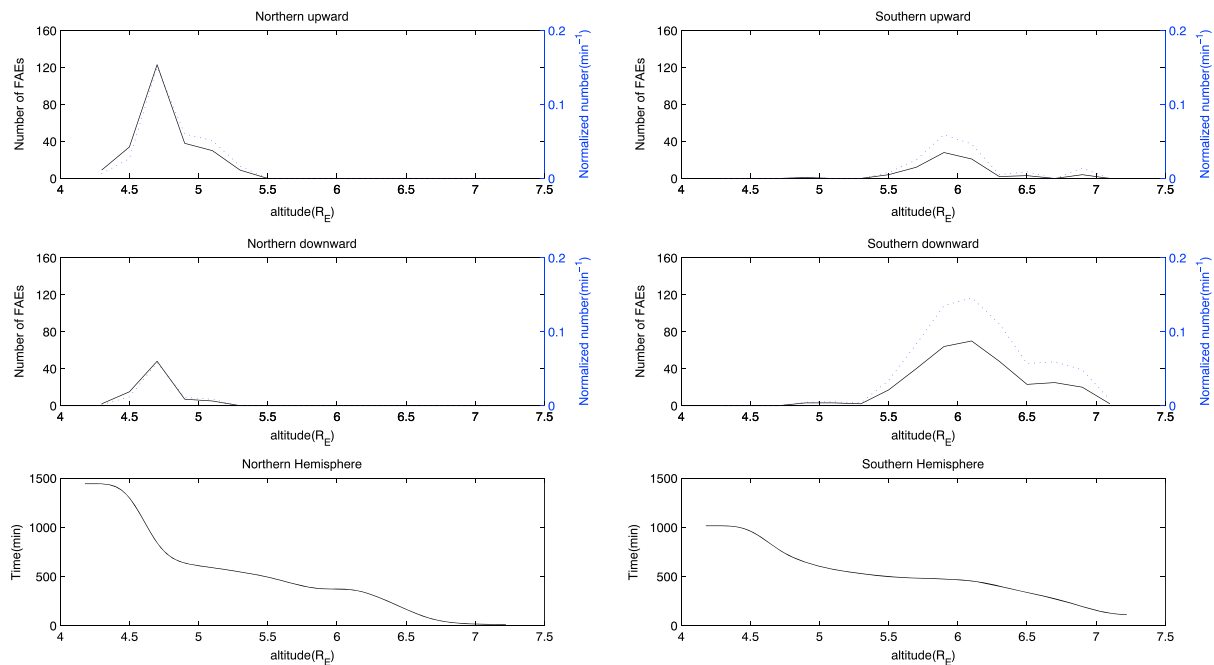


**Figure 4.** Field-aligned electron (FAE) events number (black, full lines) and the normalized number (blue, dashed lines) versus altitude in both cusp regions. The upper panels are for the upward, the middle panels are for the downward, and the lower panels are the number of minutes that Cluster spent in each altitude bin. All the data are limited to 0900–1500 magnetic local time in 2003 and 2004. The left column is for the Northern Hemisphere, and the right column is for the Southern Hemisphere.

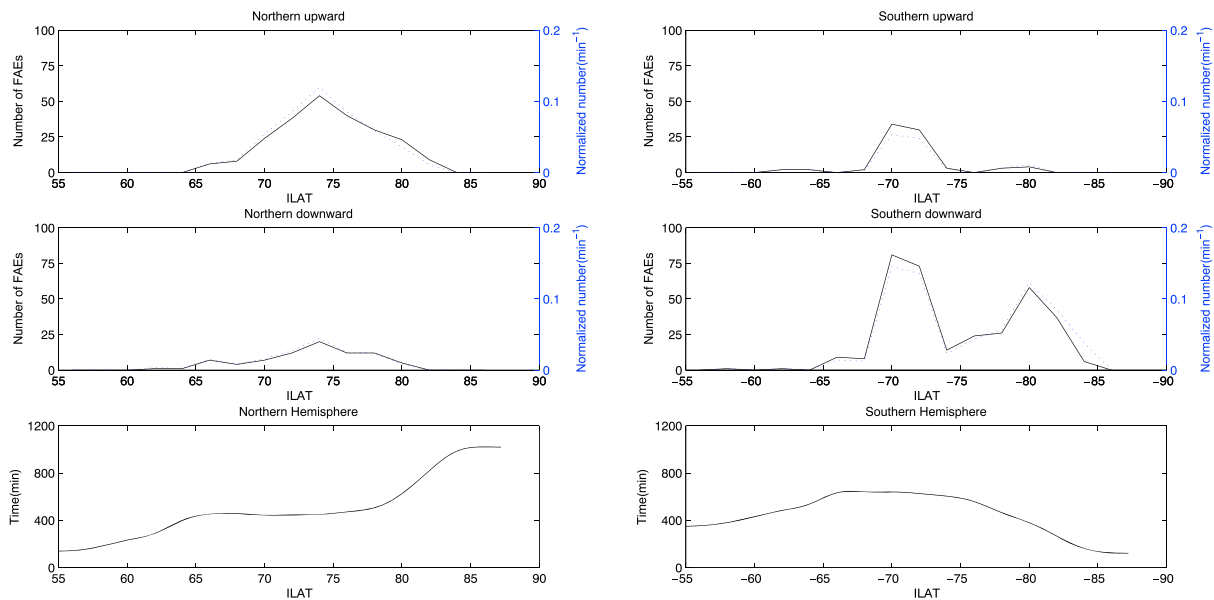


**Figure 5.** Field-aligned electron (FAE) events number (black, full lines) and the normalized number (blue, dashed lines) versus invariant latitude (ILAT) in both cusp regions. The upper panels are for the upward, the middle panels are for the downward, and the lower panels are the number of minutes that Cluster spent in each ILAT bin. All the data are limited to 0900–1500 magnetic local time in 2003 and 2004. The left column is for the Northern Hemisphere, and the right one is for the Southern Hemisphere.

The lower panel in Figure 4 gives the number of minutes that Cluster spent in each altitude bin. The normalized number of the FAE events is defined as the number of the FAE events divided by the number of minutes that Cluster spent in each altitude bin. We can see that, versus altitude, the features of the FAE events distributions and the normalized distributions are near the same. From both the FAE events and the normalized events distribution, we can see that around the northern cusp both the upward and downward FAEs are distributed in the altitude range of  $4.3$  to  $5.5 R_E$  with a peak at about  $4.7 R_E$ , and around the southern cusp both the upward and downward FAEs are distributed in the altitude range of  $4.5$  to  $7.5 R_E$  with a peak at about  $6 R_E$ . For both upward and downward FAEs, the peak altitude around the northern cusp is about  $1.3 R_E$  lower than that around the southern cusp.

From Figure 4, we also can see that in the Southern Hemisphere the downward FAE events dominate and have their peak at about  $6 R_E$ , whereas in the northern cusp we notice that upward FAE events prevail with a peak at about  $4.7 R_E$ .

Hereby, we conclude that the altitude distribution of the FAE events at high altitude (at the Cluster orbit) around the two cusp regions display an obvious asymmetry between the Southern and Northern Hemispheres. (The orbit effect on the asymmetry will be discussed later.)

### 3.3. ILAT Distribution in Both Hemispheres

The upper and middle panels in Figure 5 depict the distribution of FAE events (with event number and normalized number) versus ILAT around the cusp region both in the Southern and Northern Hemispheres. The lower panels in Figure 5 gives the number of minutes that Cluster spent in each ILAT bin. The normalized number is defined as the number of the FAEs events divides the number of minutes that Cluster spent in each ILAT bin. We can see that, versus ILAT, the features of the FAE events distribution and the normalized distribution are also nearly the same. From both the FAE events and the normalized distribution, we can see that around the southern cusp the upward FAE events had only one remarkable peak at about  $69^\circ$  ILAT. For the downward FAE events, there were two remarkable peaks, the main one at about  $69^\circ$  and another one at about  $81^\circ$ . Around the northern cusp region, the ILAT distribution of the FAE events had only one remarkable peak for both directions at about  $74^\circ$ . The main peaks in the Southern Hemisphere were  $5^\circ$  lower than in the Northern Hemisphere.

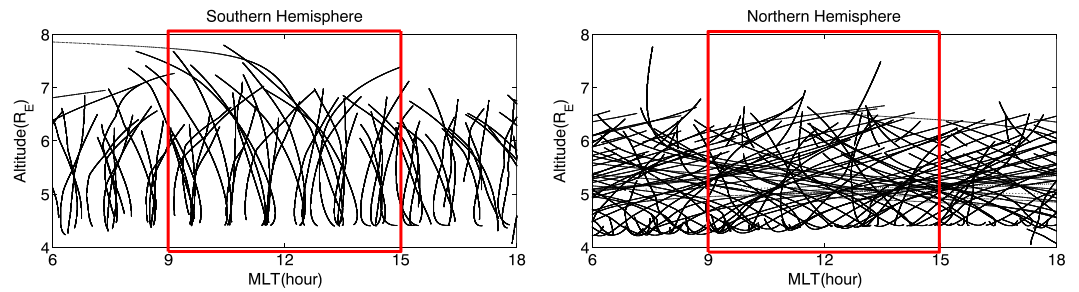


**Figure 6.** Distribution of the Cluster C3 satellite orbit in the magnetic local time (MLT)-altitude plane in northern (left panel) and southern polar regions (right panel) in 2003 and 2004. The cusp region lies in the MLT range 0900–1500.

For further comparison, we can see that the distribution of downward FAE events around the cusp in the Southern Hemisphere was much different from that in the northern. Furthermore, the number of the FAE events around the second peak in the Southern Hemisphere exceeded the number of all downward FAE events around the northern cusp.

Therefore, we can say that there was a northern-southern hemispheric asymmetry in the FAE events distribution versus the ILAT around the two cusp regions.

As a conclusion for the above, the FAE events observed around the two cusp regions display a north-south asymmetry in the FAE events distribution and normalized distribution. The asymmetry appeared in the altitude distribution and also in the ILAT distribution, both for the upward and the downward FAEs.

#### 4. Discussion

When considering the north-south asymmetry of the FAE events distribution around the cusp regions, the primary attention should be on the influence of satellite orbit. Indeed, the Cluster C3 satellite crossed the northern and southern cusp regions at slightly different altitudes. In 2003 and 2004, it crossed the cusp region at the altitude range of  $4.2\text{--}7.1 R_E$  in the south and  $4.2\text{--}6.7 R_E$  in the north. Therefore, the Cluster orbit certainly has an influence on the distribution, but we argue in the following that the asymmetry of the FAE events distribution around the cusp region should not be totally influenced by the satellite orbit.

Figure 6 shows the Cluster C3 orbit coverage of the entire polar region in the Northern and Southern Hemispheres in 2003 and 2004. The cusp region is defined as the MLT range 0900–1500. We can see that the satellite orbit coverage was relatively uniform in the whole polar region.

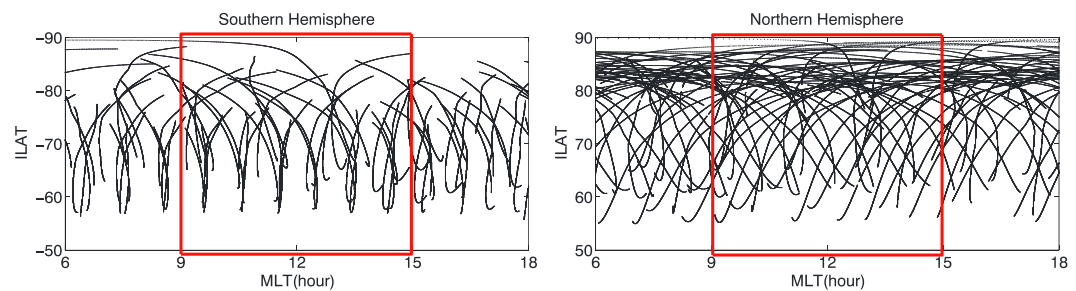
We can see that the lower boundary of the altitude range of the C3 satellite orbits around the northern cusp was the same as that around the southern cusp. The upper boundary of the altitude range of C3 satellite orbits was about  $7.1 R_E$  for the southern cusp and about  $6.7 R_E$  for the northern cusp. The difference was only  $0.4 R_E$ . The average altitude is about  $5.65 R_E$  around the northern cusp and about  $5.45 R_E$  around the southern cusp. The difference was only  $0.2 R_E$ .

Table 2 lists some key parameters for the characteristics of the FAE distribution for the upward and the downward events around the cusp region in both the Southern and Northern Hemispheres.

**Table 2**  
C3 Orbit and FAE Events Distribution With Altitude Around the Two Cusps

Two cusps	C3 orbit altitude		Upward FAE events		Downward FAE events	
	Range	Average	Number	Peak at	Number	Peak at
Southern cusp	$4.2\text{--}7.1 R_E$	$5.65 R_E$	75	$5.9 R_E$	317	$6.1 R_E$
Northern cusp	$4.2\text{--}6.7 R_E$	$5.45 R_E$	243	$4.7 R_E$	77	$4.7 R_E$
Difference	$0.0\text{--}0.4 R_E$	$0.2 R_E$	—	$1.2 R_E$	—	$1.4 R_E$

Note. FAE = field-aligned electron.



**Figure 7.** Distribution of the Cluster C3 orbit in the magnetic local time (MLT)-invariant latitude (ILAT) plane in the southern (left panel) and northern (right panel) polar region in 2003 and 2004. The cusp region is limited by MLT 0900–1500.

We can compare the orbit coverage in Figure 6 with the FAE events distribution and the normalized number distribution shown in Figure 4 and Table 2. Both for the upward and downward directions, the FAE events around the cusp region concentrated around  $6 R_E$  in the Southern Hemisphere and around  $4.7 R_E$  in the northern one. The altitude difference of the FAEs peaks both for the upward and downward was about  $1.2\text{--}1.4 R_E$  and exceeds the hemispheric differences of the orbit distributions. Therefore, we conclude that there was indeed a north-south asymmetry of the FAE events distribution around the two cusps, both for the upward and the downward directions.

From Table 2, we can see that the downward FAE events were mainly observed around the southern cusp region and at higher altitude (with an average of  $6.1 R_E$ ), and the upward FAE events were mainly observed around the northern cusp region (with an average of  $4.7 R_E$ ). This difference in the altitude distribution is consistent with previous observations that the downward FAEs prevail at higher altitudes and the upward FAEs at lower ones (Shi et al., 2017; Yoshioka et al., 2000).

Based on previous literature, we also can say that the high number of FAE events observed at higher altitude in the Southern Hemisphere was mainly influenced by the solar wind electron injection and that the high number of FAE events observed at lower altitude in the Northern Hemisphere was mainly influenced by the upstreaming of ionospheric electrons. So it is easy to understand that there were more downward FAE events around the southern cusp region with higher latitude, and there were more upward FAE events around the northern cusp region with lower altitude.

To discuss the FAEs distribution versus ILAT (in Figure 5), where the downward FAE events around the southern cusp show a second peak at ILAT  $81^\circ$ , we have checked the data with the Cluster orbit. Figure 7 illustrates the Cluster C3 orbit coverage in the MLT-ILAT plane in the northern and southern polar regions in 2003 and 2004. The cusp region is limited by MLT 0900–1500.

Comparing the two hemispheres, we can see that the C3 orbit coverage at ILAT from  $78\text{--}88^\circ$  was much denser in the Northern Hemisphere, but the second peak of the FAE events for the downward FAEs in the Southern Hemisphere was at ILAT  $81^\circ$ . This further demonstrates that the observed north-south asymmetry of the FAE events distribution versus ILAT.

We have checked the downward FAE events in the southern cusp around the second peak (see Figure 5). The total number of the FAE events around the second peak was 132. There were 102 events located at ILAT  $> 77^\circ$ , and they occurred with solar wind speeds greater than 500 km/s and geomagnetic activity index  $K_p > 4$ . This suggests that during high solar wind speed and higher geomagnetic activity, there would be more solar wind electrons entering the cusp, resulting in more frequent downward FAE events in the higher ILAT range in southern cusp region. Therefore, we can understand that the second peak of the downward FAE events distribution versus ILAT around the southern cusp was associated with high solar wind speed and high geomagnetic activity. The second peak was only found in the Southern Hemisphere, which shows that the Southern Hemisphere at higher altitudes is more susceptible to solar wind (while the Northern Hemisphere seemed to be less susceptible to solar wind).

As we know, FAEs are tightly associated with the FAC and are carriers of the FACs in the polar region (Berko et al., 1975; Morooka et al., 1998). So FAEs can be seen as a signal of the FAC. Some authors

studied the FAC in the dayside auroral region at low altitude and found that when the northward interplanetary magnetic field (IMF)  $B_z$  is strong enough, a new FAC called NBZ (northward IMF  $B_z$ ) current can be formed outside the poleward boundary of the Region 1 FAC. That is, the NBZ currents are separated from the Region 1 FAC (Iijima et al., 1984). A subsequent study showed that the NBZ FAC occurs not only in the auroral region but also on the nightside and with a complex structure (Iijima & Shibaji, 1987). The second peak (at ILAT 81°) of the downward FAE events (corresponding to an outflowing FAC) shown in Figure 5 in the Southern Hemisphere was separated from the main peak (at ILAT 69°) and may be associated with the NBZ FAC at low altitude, but it is at higher altitude. With the Swarm observations at the altitude of 420 km (Huang et al., 2017; Lühr et al., 2015), found that the NBZ current in the Southern Hemisphere corresponds to negative IMF  $B_y$ . In our study, with Cluster observation at the altitude of 4–7  $R_E$ , most of the FAE events around the second peak in Figure 5 corresponded to positive IMF  $B_y$ , and the altitude of the observation was much higher than that of Swarm. Therefore, the correlation between the NBZ current and the FAEs event at high ILAT in the south hemisphere in this study needs to be further studied with more observations and theoretical analysis.

From the Table 1 and Figure 4, we can see that the downward FAEs event number in the north fits better to the number of upward events in the south. This is similarly true for the opposite flow direction. Since the data used in this study were from late summer and early autumn in the north (late July to early October), which corresponded to late winter and early spring in the south, they indicated clearly seasonal effect. This is consistent with the study by Laundal et al. (2018) finding that the FACs in the two hemispheres were not the same because of the seasonal influence. For further analysis, we have split the observation period into two parts, July–August (northern late summer) and September–October (northern early autumn). The results show that in both the period of July–August and September–October, the downward event number in the north fits better to the number of upward events in the south, also for the opposite flow direction. In this view, it seems that there was no clear difference in the FAEs distributions in the two periods. However, this needs to be further studied.

The results of this paper suggest a north-south hemispheric asymmetry of the FAE events distribution around the two cusp regions. The asymmetry could be associated to several plausible causes. Because of interaction with the magnetosphere, solar wind has a controlling role to the cusp location and to the current in the polar region (Candidi et al., 1989; Huang et al., 2017; Smith & Lockwood, 1996). As we know, the geomagnetic dipole moment has a tilt angle of 11° with the Earth's spin axis and the solar wind flow with its dynamic pressure has asymmetry relating to the magnetosphere (Hedgecock & Thomas, 1975). They can result in a north-south hemispheric asymmetry of the cusp location in the magnetosphere (Nemecek et al., 2000; Smith & Lockwood, 1996) and also result in an FAE event asymmetry between the northern and southern cusps. Therefore, the magnetospheric configuration should be the first cause of the asymmetry of the FAEs around the two cusps.

Some authors studied the IMF  $B_y$  influence on the magnetosphere (Burch et al., 1985; Cowley, 1981; Greenwald et al., 1990). The results show that the IMF  $B_y$  can also result in the asymmetry in the two hemispheres. The IMF  $B_y$  can produce a curvature of geomagnetic field lines such that they are subject to a tension force in the  $Z$  and  $Y$  directions. For positive  $B_y$ , the field lines move toward dawn in the Northern Hemisphere and toward dusk in the Southern Hemisphere. The directions are reversed for negative  $B_y$ . In the ionosphere this movement maps to eastward or westward flows, which have opposite directions in the two hemispheres and the directions depend upon the IMF  $B_y$  (Cowley, 1981; Greenwald et al., 1990). Therefore, the IMF  $B_y$  is also a cause of the asymmetry of the FAEs distribution in the two cusps.

Fujii et al. (1981) studied the seasonal dependence of large-scale Birkeland currents. They showed that the ionospheric conductivity is also responsible for the asymmetry in the two hemispheres. Ohtani et al. (2005) studied the variations of the location and intensity of large-scale currents. They argued that since there is a dipole tilt angle in the magnetosphere, the distributions of ionospheric conductivity in the two hemispheres differ because of different solar extreme ultraviolet radiation fluxes reaching the two hemispheres, which will result in differences in the ionization rate and charged particle density in the ionosphere. Therefore, the difference of the ionospheric conductivity, indeed, the difference of the charged particle densities in the two hemispheres (Vallat et al., 2005), can result in hemispheric asymmetry. Christiansen et al. (2002) found that the field-aligned intensities at high latitude in summer polar cap can exceed those in



winter by a factor of 1.5 to 1.8, which gives evidence to support the north-south hemispheric asymmetry. Thus, we can say that the ionospheric conductivity is another cause for the FAEs asymmetry in the two cusps.

In the magnetosphere-ionosphere coupling system, the FAC also displays a north-south asymmetry in the magnetosphere (Huang et al., 2017; Shi et al., 2010). Christiansen et al. (2002) studied seasonal variations of high-latitude FACs inferred from Ørsted and Magsat observations. They argued that the seasonal dependence in the global FAC system is also generated and maintained by various solar wind-magnetosphere interaction processes, such as quasi-viscous interaction and reconnection (Holzer & Slavin, 1979). Hereby, since the electrons are the main carriers of the FACs, the north-south hemispheric asymmetry of the FAE events around the cusp regions can also be understood with that argument by Christiansen et al. (2002).

However, the north-south hemispheric asymmetry of the FAE events around the two cusp regions needs to be further investigated, both by observation and theoretical study.

## 5. Summary

In this paper, the characteristics of the distribution of the FAE events around the polar cusp region in the Northern and Southern Hemispheres are statistically studied. The data were taken from the instruments PEACE and FGM onboard the Cluster C3 satellite and were observed from late July to early October in 2003 to 2004. We selected electrons with field-aligned flux greater than  $3 \times 10^8 \text{ (cm}^2 \text{ s)}^{-1}$  as FAE event and divided the FAE events into upward and downward events.

The results in this study are as follows. The total numbers of FAE events (or FAE occurrences) observed around the cusp region in the Northern and Southern Hemispheres were basically identical, but there were more downward FAE events in the south and more upward FAE events in the north. The peak of the altitude distribution of the FAE events observed around the southern cusp was about  $1.3 R_E$  higher than that observed around the northern cusp. The peak of the ILAT distribution of the FAE events observed around the southern cusp was about  $5^\circ$  lower than that observed around the northern cusp. Only for downward FAEs around the southern cusp, there was a second ILAT peak at an altitude about  $11^\circ$  higher than that of the main peak. We also performed an analysis using the normalized FAE number, which is the number of the FAE events divided by the number of minutes that Cluster spent in each concerned bin. The number of normalized FAE events showed nearly the same features as the number of unnormalized FAE events. Therefore, our results indicated a clear north-south asymmetry in the FAE distribution around the two cusp regions.

We have split the observations into summer period (July–August) and autumn period (September–October). It seemed that there was no clearly difference in the FAEs distributions in the two periods. However, this needs to be further studied based on more observations.

In order to understand the mechanism of the north-south asymmetry of the FAE events around the two cusps, we analyzed the Cluster orbit coverage in the two hemispheres. The results showed that the different orbit coverage in the two hemispheres did have some influence on the asymmetry of the FAE events distribution with altitude, but it was not enough to explain the difference of the FAEs in the two hemispheres. The main causes for the asymmetry of the FAE events around the two cusps are discussed. The magnetospheric configuration, especially the geomagnetic dipolar tilt angle and the solar wind flow, is the first one. Second, the IMF orientation related to the magnetosphere can also result in asymmetry. Third, the difference of ionospheric conductivity distributions in the two hemispheres resulting from different extreme ultraviolet radiation in the summer and winter polar cap was another cause for the asymmetry. Furthermore, the various solar wind-magnetosphere interaction processes, such as the quasi-viscous interaction and reconnection, certainly have some effect on the north-south hemispheric asymmetry of the FAE events distribution around the cusp regions.

The second peak of the downward FAE events distribution versus ILAT around the southern cusp was associated with high solar wind speed, which showed that the Southern Hemisphere is more susceptible to solar wind at higher altitudes. Also, it may be associated with the NBZ FAC at low altitude. This needs to be studied further.

**Acknowledgments**

This research was supported by the National Natural Science Foundation of China (41674145 and 41874172), the General Project of Science and Technology Program of Beijing Education Commission (KM201911417015), and the Specialized Research Fund for State Key Laboratory in China. We thank the PEACE and FGM instrument teams and Cluster Science Archive system providing the data on the website ([www.cosmos.esa.int/web/csa](http://www.cosmos.esa.int/web/csa)).

**References**

Balogh, A., Carr, C. M., Acuña, M. H., Dunlop, M. W., Beek, T. J., Brown, P., & Oddy, T. (2001). The cluster magnetic field investigation: Overview of in-flight performance and initial results. *Annales Geophysicae*, *19*(10/12), 1207–1217. <https://doi.org/10.5194/angeo-19-1207-2001>

Berko, F. W. (1973). Distributions and characteristics of high-latitude field-aligned electron precipitation. *Journal of Geophysical Research*, *78*(10), 1615–1626. <https://doi.org/10.1029/JA078i010p01615>

Berko, F. W., Hoffman, R. A., Burton, R. K., & Holzer, R. E. (1975). Simultaneous particle and field observations of field-aligned currents. *Journal of Geophysical Research*, *80*(1), 37–46. <https://doi.org/10.1029/JA080i001p00037>

Burch, J. L., Reiff, P. H., Menietti, J. D., Heelis, R. A., Hanson, W. B., Shawhan, S. D., et al. (1985). IMF By-dependent plasma flow and Birkeland currents in the dayside magnetosphere, 1, Dynamics Explorer observations. *Journal of Geophysical Research*, *90*(A2), 1577. <https://doi.org/10.1029/JA090iA02p01577>

Burch, J. L., Reiff, P. H., & Sugiura, M. (1983). Upward electron beams measured by DE-1: a primary source of dayside region-1 Birkeland currents. *Journal of Geophysical Research*, *10*(8), 753–756. <https://doi.org/10.1029/GL010i008p00753>

Candidi, M., Mastrantonio, G., Orsini, S., & Meng, C.-I. (1989). Evidence for the influence of the interplanetary magnetic field azimuthal component on the polar cusp configuration. *Journal of Geophysical Research*, *94*(A10), 13,585. <https://doi.org/10.1029/JA094iA10p13585>

Carlson, C. W., McFadden, J. P., Ergun, R. E., Temerin, M., Peria, W., Mozer, F. S., et al. (1998). FAST observations in the downward auroral current region: Energetic upgoing electron beams, parallel potential drops, and ion heating. *Geophysical Research Letters*, *25*(12), 2017–2020. <https://doi.org/10.1029/98GL00851>

Christiansen, F., Papitashvili, V. O., & Neubert, T. (2002). Seasonal variations of high-latitude field-aligned currents inferred from Ørsted and Magsat observations. *Journal of Geophysical Research*, *107*(A2), 1029. <https://doi.org/10.1029/2001JA900104>

Collin, H. L., Sharp, R. D., & Shelley, E. G. (1982). The occurrence and characteristics of electron beams over the polar regions. *Journal of Geophysical Research*, *87*(A9), 7504–7511. <https://doi.org/10.1029/JA087iA09p07504>

Cowley, S. W. H. (1981). Magnetospheric asymmetries associated with the Y-component of the IMF. *Planetary and Space Science*, *29*(1), 79–96. [https://doi.org/10.1016/0032-0633\(81\)90141-0](https://doi.org/10.1016/0032-0633(81)90141-0)

Escoubet, C. P., Fehringer, M., Goldstein, M., & (2001). The Cluster mission. *Annales Geophysicae*, *19*(10/12), 1197–1200. <https://doi.org/10.5194/angeo-19-1197-2001>

Fujii, R., Iijima, T., Potemra, T. A., & Sugiura, M. (1981). Seasonal dependence of large-scale Birkeland currents. *Geophysical Research Letters*, *8*(10), 1105–1106.

Greenwald, R. A., Baker, K. B., Ruohoniemi, J. M., Dudeney, J. R., Pinnock, M., Mattin, N., et al. (1990). Simultaneous conjugate observations of dynamic variations in high-latitude dayside convection due to changes in IMF By. *Journal of Geophysical Research*, *95*(A6), 8057. <https://doi.org/10.1029/JA095iA06p08057>

Hedgcock, P. C., & Thomas, B. T. (1975). Heos observations of the configuration of the magnetosphere. *Geophysical Journal of the Royal Astronomical Society*, *41*(3), 391–403. <https://doi.org/10.1111/j.1365-246X.1975.tb01622.x>

Hoffman, R. A., & Evans, D. S. (1968). Field-aligned electron bursts at high latitudes observed by OGO 4. *Journal of Geophysical Research*, *73*(19), 6201–6214. <https://doi.org/10.1029/JA073i019p06201>

Holzer, T. E., & Slavin, J. A. (1979). Magnetic flux transfer associated with expansions and contractions of the dayside magnetosphere. *Journal of Geophysical Research*, *83*(A8), 3831–3839.

Hu, R., Bogdanova, Y. V., Owen, C. J., Foullon, C., Fazakerley, A. N., & Rème, H. (2008). Cluster observations of the midaltitude cusp under strong northward interplanetary magnetic field. *Journal of Geophysical Research*, *113*, A7, A07S05. <https://doi.org/10.1029/2007JA012726>

Huang, T., Lühr, H., & Wang, H. (2017). Global characteristics of auroral Hall currents derived from the Swarm constellation: dependences on season and IMF orientation. *Annales Geophysicae*, *35*, 1249–1268. <https://doi.org/10.5194/angeo-35-1249-2017>

Iijima, T., Potemra, T. A., Zanetti, L. J., & Bythrow, P. F. (1984). Large-scale Birkeland currents in the dayside polar region during strongly northward IMF: A new Birkeland current system. *Journal of Geophysical Research*, *89*(A9), 7441–7452. <https://doi.org/10.1029/JA089iA09p07441>

Iijima, T., & Shibaji, T. (1987). Global characteristics of northward IMF associated (NBZ) field-aligned currents. *Journal of Geophysical Research*, *92*, 2408–2424. <https://doi.org/10.1029/JA092iA03p02408>

Johnstone, A. D., Alsop, C., Burge, S., Carter, P. J., Coates, A. J., Coker, A. J., & Woodliffe, R. D. (1997). PEACE: A Plasma Electron and Current Experiment. *Space Science Reviews*, *79*(1/2), 351–398. <https://doi.org/10.1023/A:1004938001388>

Johnstone, A. D., N. J. Flowers, and R. Liu (1994). Observations in the equatorial region of the field-aligned electron and ion distributions in the energy range 100 eV to 5 keV associated with substorm onsets, in Proceedings of the Second International Conference on Substorms, Fairbanks, Alaska, Geophys. Inst., Univ. of Alaska, Fairbanks, Alaska.

Johnstone, A. D., & Winningham, J. D. (1982). Satellite observations of suprathermal electron bursts. *Journal of Geophysical Research*, *87*(A4), 2321–2329. <https://doi.org/10.1029/JA087iA04p02321>

Kintner, P. M., Ackerson, K. L., Gurnett, D. A., & Frank, L. A. (1978). Correlated Electric Field and Low-Energy Electron Measurements in the Low-Altitude Polar Cusp. *Journal of Geophysical Research*, *83*(A1), 163–168. <https://doi.org/10.1029/JA083iA01p00163>

Laundal, K. M., Finlay, C. C., Olsen, N., & Reistad, J. P. (2018). Solar wind and seasonal influence on ionospheric currents from Swarm and CHAMP measurements. *Journal of Geophysical Research: Space Physics*, *123*, 4402–4429. <https://doi.org/10.1029/2018JA025387>

Lin, C. S., & Hoffman, R. A. (1979). Fluctuations of inverted V electron fluxes. *Journal of Geophysical Research*, *84*(A11), 6547–6553. <https://doi.org/10.1029/JA084iA11p06547>

Lühr, H., Park, J., Gjerloev, J. W., Rauberg, J., Michaelis, I., Merayo, J. M. G., & Brauer, P. (2015). Field-aligned currents' scale analysis performed with the Swarm constellation. *Geophysical Research Letters*, *42*, 1–8. <https://doi.org/10.1002/2014GL062453>

Ma, Y. D., Cao, J. B., Nakamura, R., Zhang, T. L., Rème, H., Dandouras, I., et al. (2009). Statistical analysis of earthward flow bursts in the inner plasma sheet during substorms. *Journal of Geophysical Research*, *114*, A07215. <https://doi.org/10.1029/2009JA014275>

Miyake, W., Mukai, T., & Kaya, N. (1998). A statistical study of field-aligned electron beams associated with ion conics events. *Annales Geophysicae*, *16*(8), 940–947. <https://doi.org/10.1007/s00585-998-0940-x>

Morooka, M., Yamamoto, T., Mukai, T., Tsuruda, K., Hayakawa, H., & Fukunishi, H. (1998). In S. Ko-kubun, & Y. Kamide (Eds.), *Relationship between field-aligned currents and parallel electric field observed by Akebono, in Substorms-4*, (Vol. 59, –62). Norwell, Mass: Kluwer Acad.

Nemecek, Z., Měrka, J., & Šafránková, J. (2000). The tilt angle control of the outer cusp position. *Geophysical Research Letters*, *27*(1), 77–80. <https://doi.org/10.1029/1999GL010699>

- Ohtani, S., Ueno, G., Higuchi, T., & Kawano, H. (2005). Annual and semi-annual variations of the location and intensity of large-scale field-aligned currents. *Journal of Geophysical Research*, *110*, A01216. <https://doi.org/10.1029/2004JA010634>
- Sharp, R. D., Shelley, E. G., Johnson, R. G., & Ghielmetti, A. G. (1980). Counterstreaming electron beams at altitudes of  $\sim 1 R_E$  over the auroral zone. *Journal of Geophysical Research*, *85*(A1), 92–100. <https://doi.org/10.1029/JA085iA01p00092>
- Shi, J., Zhang, Z., Torkar, K., Cheng, Z., Farzakeley, A., Dunlop, M., & Carr, C. (2017). Distribution of field-aligned electron events in the high-altitude polar region: Cluster observations. *Journal of Geophysical Research: Space Physics*, *122*, –11,245, 11,255. <https://doi.org/10.1002/2017JA024360>
- Shi, J., Zhang, Z., Torkar, K., Dunlop, M., Fazakerley, A., Cheng, Z., & Liu, Z. (2014). Temporal and spatial scales of a high-flux electron disturbance in the cusp region: Cluster observations. *Journal of Geophysical Research: Space Physics*, *119*, 4536–4543. <https://doi.org/10.1002/2013JA019560>
- Shi, J. K., Cheng, Z. W., Zhang, T. L., Dunlop, M., Liu, Z. X., Torkar, K., et al. (2010). South-north asymmetry of field-aligned currents in the magnetotail observed by Cluster. *Journal of Geophysical Research*, *115*, A07228. <https://doi.org/10.1029/2009JA014446>
- Smith, M. F., & Lockwood, M. (1996). Earth's magnetospheric cusps. *Review of Geophysics*, *34*(2), 233–260. <https://doi.org/10.1029/96RG00893>
- Thelin, B., & Lundin, R. (1990). Upflowing ionospheric ions and electrons in the cusp-cleft region. *Journal of Geomagnetism and Geoelectricity*, *42*(6), 753–761. <https://doi.org/10.5636/jgg.42.753>
- Torbert, R. B., & Carlson, C. W. (1980). Evidence for parallel electric field particle acceleration in the dayside auroral oval. *Journal of Geophysical Research*, *85*(A6), 2909–2914. <https://doi.org/10.1029/JA085iA06p02909>
- Tsyganenko, N. A., & Stern, D. P. (1996). Modeling the global magnetic field of the large-scale Birkeland current systems. *Journal of Geophysical Research*, *101*(A12), 27,187–27,198. <https://doi.org/10.1029/96JA02735>
- Vallat, C., Dandouras, I., Dunlop, M., Balogh, A., Lucek, E., Parks, G. K., et al. (2005). First current density measurements in the ring current region using simultaneous multi-spacecraft Cluster-FGM data. *Annales Geophysicae*, *23*(5), 1849–1865. <https://doi.org/10.5194/angeo-23-1849-2005>
- Yoshioka, R., Miyake, W., Mukai, T., & Ito, M. (2000). Field-aligned electron beams observed simultaneously with upflowing ion beams in the auroral acceleration region. *Journal of Geophysical Research*, *105*(A4), 7679–7694. <https://doi.org/10.1029/1999JA900486>
- Zanetti, L. J., Potemra, T. A., Doering, J. P., & Lee, J. S. (1981). Magnetic field-aligned electron distributions in the dayside cusp. *Journal of Geophysical Research*, *86*(A11), 8957–8970. <https://doi.org/10.1029/JA086iA11p08957>